Journal of Nuclear Medicine, published on July 17, 2020 as doi:10.2967/jnumed.120.245530

A microdosing study with 99mTc-PHC-102 for the SPECT/CT imaging of primary and metastatic lesions in renal cell carcinoma patients

Oana C. Kulterer[1•], Sarah Pfaff[1], Wolfgang Wadsak[1,2], Nathalie Garstka[3], Mesut Remzi[3], Chrysoula Vraka[1], Lukas Nics[1], Franziska Bootz[4], Samuele Cazzamalli[4], Nikolaus Krall[5], Dario Neri[6] and Alexander R. Haug[1,7]*

1) Department of Biomedical Imaging and Image-guided Therapy, Division of General and Pediatric Radiology, Medical University of Vienna, Waehringer Guertel 18-20, 1090, Vienna, Austria

2) Center of Biomarker Research in Medicine – CBmed, Stiftingtalstrasse 5, 8010 Graz, Austria

3) Department of Urology, Medical University of Vienna, Waehringer Guertel 18-20, 1090, Vienna, Austria

4) Philochem AG, Libernstrasse 3, CH-8112 Otelfingen (Switzerland)

5) Allcyte GmbH, Campus Vienna Biocenter 5, A-1030 Vienna (Austria)

6) Department of Chemistry and Applied Biosciences, ETH Zürich, Vladimir-Prelog-Weg 4, CH-8093 Zürich

7) Christian Doppler Laboratory for Applied Metabolomics, Medical University of Vienna, Waehringer Guertel 18-20, 1090, Vienna, Austria

•) First Author

Oana C. Kulterer

Division of Nuclear Medicine

Department of Biomedical Imaging and Image-guided Therapy

Medical University of Vienna

1090 Vienna, Austria.

Tel.: +43 40400 58740

Fax: +43 40400 55320

e-mail: oana.kulterer@meduniwien.ac.at

*) Corresponding Author

Alexander R. Haug

Division of Nuclear Medicine

Department of Biomedical Imaging and Image-guided Therapy

Medical University of Vienna

1090 Vienna, Austria.

Tel.: +4314040039360

Fax: +4314040055320

e-mail: alexander.haug@meduniwien.ac.at

Financial Support

This project has received funding from the European Community under the grant agreement number E!9669 ATRI. D.N. was supported by ETH Zurich. This project has received funding from the Swiss National Science Foundation (Grant Nr. 310030_182003/1) and the European Research Council (ERC) under the European Union's Horizon 2020 research and innovation program (grant agreement 670603).

Disclosure of Potential Conflict of Interest

D.N. is co-founder and shareholder of Philogen S.p.A. (www.philogen.com), a Swiss-Italian Biotech company that owns PHC-102. S.C. is an employee of Philochem AG. N.K. is entitled to shares

of licensing revenues from ETH for PHC-102. No other potential conflicts of interest relevant to this article exist.

Short Running Title

99mTc-PHC-102 SPECT in RCC

Submitted to the *Journal of Nuclear Medicine* as an Original Research Article

Authors confirm that data presented in tables and figures are accurate

ABSTRACT

99mTc-PHC-102 is a 99mTc-labeled derivative of acetazolamide, a high-affinity small organic ligand of Carbonic Anhydrase IX (CAIX). 99mTc-PHC-102 has previously shown favourable *in vivo* biodistribution properties in mouse models of CAIX-positive clear cell renal cell carcinoma (ccRCC) and colorectal cancer. In this study, we aimed to explore the targeting performance of 99mTc-PHC-102 in single-photon emission computed tomography (SPECT) in patients with RCC, while also assessing the safety and tolerability of the radiotracer.

Methods We studied five patients with localized or metastatic clear cell renal cell carcinoma (ccRCC) in a microdosing regimen, after the administration of 50 µg total CAIX ligand and 600-800 MBq 99mTc-PHC-102. Tissue distribution and residence time in normal organs and tumors were analysed by serial SPECT/CT scans at three time points (30 minutes, 2, and 6 hours) after intravenous administration.

Results In the five patients studied, 99mTc-PHC-102 was well tolerated and no study drug-related adverse events were recorded. The radiotracer showed a rapid initial uptake in the stomach, kidneys and gallbladder, which cleared over time. Localization of the study drug in primary tumors of five patients was observed with favourable tumour-to-background ratios. 99mTc-PHC-102 -SPECT/CT allowed the identification of four previously unknown lung and lymph node metastases in two patients.

Conclusions 99mTc-PHC-102 is a promising SPECT tracer for the imaging of patients with clear cell renal cell carcinoma. This tracer has the potential to identify primary and metastatic lesions in different anatomical locations. 99mTc-PHC-102 might also serve as companion diagnostic agent for future CAIX-targeting therapeutics.

Keywords clear cell renal cell carcinoma, carbonic anhydrase IX, Single-Photon Emission Computed Tomography, 99mTc, PHC-102

INTRODUCTION

Carbonic anhydrase IX (CAIX) is a membrane-bound metalloenzyme involved in the maintenance of cellular acid–base homeostasis. CAIX is almost undetectable in normal adult tissues, with the exception of certain organs of the gastrointestinal tract [1-3]. This enzyme is nonetheless strongly expressed in most clear cell renal cell carcinomas (ccRCCs), as a result of von Hippel–Lindau mutations or deletions [4]. Furthermore, at sites of hypoxia, a frequent condition in neoplastic solid masses, CAIX expression is abundant. Every year, more than 70,000 patients are diagnosed with kidney cancer in the United States, with a mortality rate of around 14,000 cases per year (www.cancer.gov). The majority of ccRCCs are CAIX-positive and hence, provide an ideal target for imaging and drug delivery applications [5]. In principle, CAIX-ligands could be used to deliver radionuclides to the tumor site for imaging applications and/or for targeted radionuclide therapy [6, 7]. Moreover, CAIX ligands could be used for selective drug delivery applications, liberating cytotoxic agents at the tumor site and helping spare normal tissues [7-12].

The non-invasive detection of CAIX-positive tumors has been extensively studied by using radiolabeled preparations of the cG250 antibody. In particular, ^{124}I-labeled cG250 could be used to localized ccRCC, with a satisfying tumor-to- kidney ratio of about 3:1 [13]. Furthermore, the use of [^{124}I]I-cG250 immunoPET/CT has shown a significantly higher detection rate of ccRCC as compared to conventional CT [14]. However, intact antibodies are not ideally suited for imaging applications, as their large size and slow clearance may lead to high radiation doses for patients [13-15]. For this reason, it is desirable to target CAIX-positive tumors with radiolabeled preparations of small organic ligands, capitalizing on a better diffusion into the solid tumor mass and a faster clearance [12, 16].

Initial attempts at targeting CAIX-positive tumors with radiolabeled aromatic sulfonamide derivatives had failed to show an acceptably high enrichment in neoplastic lesions, both in mouse models of cancer [17, 18] and in patients [19]. However, our group has previously shown that acetazolamide derivatives could be used for the selective delivery of radionuclide or fluorophores for imaging applications or therapy in CAIX-positive tumors [6, 7, 8, 11, 12, 20]. The use of charged linkers helped minimize ligand internalization into cells and, consequently, the undesired targeting of intracellular carbonic anhydrases [8].

99mTc-PHC-102 is a 99mTc-labeled acetazolamide derivative; acetazolamide, is already an approved drug that is administered at doses of 0.5-1 gram per patient [21], which has shown promising biodistribution results in tumor-bearing mice [6, 7]. 99mTc is an attractive gamma-emitting radionuclide for nuclear imaging applications, in view of its short half-life (6 hours), easy production by generators [22] and tolerability [23, 24].

In this article, we aimed at assessing the safety and tolerability of 99mTc-PHC-102, while also exploring its tumor-targeting performance by single-photon emission computed tomography (SPECT) imaging in patients with localized or metastatic ccRCC. We used a microdosing approach in order to capitalize on favorable regulatory guidelines for the execution of such studies in Europe and in the United States.

MATERIAL AND METHODS

Study Design and Patient Population

This study was designed as a first-in-human, uncontrolled, single-center, single-dose, open-label, non-randomized, prospective, exploratory microdosing study with the primary objective to assess the safety and tolerability of 99mTc-PHC-102 in subjects with localized or metastatic clear cell renal cell carcinoma (ccRCC). As secondary objectives, the targeting performance in terms of biodistribution as fraction of injected activity and dosimetry (with a particular focus on tumor uptake) and pharmacokinetics was evaluated.

Five male patients, aged between 33 and 80 years (62 ± 9.2), localized or metastatic ccRCC as confirmed by CT and optional histology, scheduled for surgical resection of the primary renal mass were enrolled and imaged by SPECT/CT.

The study has received authorisation from the Austrian competent Authority (AGES/BASG) and from the Ethics Committee of the Medical University of Vienna. This trial was registered under the EUDRACT number 2016-004909-13 and was conducted in accordance with the Declaration of Helsinki with the applicable regulatory requirements for Austria, according to International Conference on Harmonisation guidelines. All subjects provided written informed consent before participating in the study.

Radiopharmaceutical Preparation

99mTc-PHC-102 consists of the clinically approved carbonic anhydrase (CA) inhibitor acetazolamide moiety linked to a peptide-based 99mTc-chelator through a triazole-aspartic acid linker. 99mTc-PHC-102 was freshly prepared from the non-radioactive precursor (PHC-101) and sodium 99mTc-pertechnetate (Na99mTc-TcO_4) under reducing conditions for each patient and was

immediately used for imaging purposes. Sodium 99mTc-pertechnetate was eluted from a commercially available and approved 99Mo/99mTc-radionuclide generator (Mallinckrodt Pharmaceuticals) using sterile, isotonic saline solution as eluent. Unlabeled precursor PHC-101 (50 µg) was dissolved in degassed TBS buffer (pH 7.4). $SnCl_2$ (200 mg) and sodium glucoheptonate (20 mg) were added followed by addition of sodium 99mTc-pertechnetate (generator eluate) in physiological saline. The reaction mixture was heated to 95°C for 20 minutes and allowed to cool to room temperature. Subsequentely, quality control was performed and pH, osmolality, radiochemical and radionuclide purity was determined.

Dosage, Administration and Dosimetry

The radiopharmaceutical 99mTc-PHC-102 was administered to the eligible patients under the supervision of the investigator and administered i.v. as a single dose bolus injection in a volume of up to 10 mL through a peripheral venous catheter. Each dose consisted of mean 729 MBq (range 608-797 MBq) of 99mTc-PHC-102 and a total amount of 50 µg of CAIX ligand (sum of radiolabeled 99mTc-PHC-102 and unlabeled PHC-101). Accurate dosimetry was performed in order to determine precise calculation of patient radiation burden from the radiopharmaceutical.

99mTc-PHC-102 SPECT/CT and Pharmacokinetic

Imaging acquisitions were performed using a SPECT/CT scanner (Symbia Intevo, Siemens Healthcare, Erlangen, Germany) 30 minutes, 2 and 6 hours post injection (a total of three scans per patient) using the xSPECT acquisition for quantitative SPECT. A low-dose CT (for attenuation correction and anatomical localization of the SPECT signal) preceded each scan. First, the whole body SPECT acquisition covering the body from the head to thighs was started followed by the low-dose CT. SPECT data were normalized and corrected for attenuation, decay and scatter. All

scans were reconstructed and optimized to get the best image quality according to the specific uptake of the radiotracer.

Pharmacokinetics were determined by drawing blood (approximatively 1 mL) from a dedicated peripheral vein site into heparin coated tubes. Blood sampling was performed 5, 10, 30 and 60 minutes as well as at 2, 4 and 6 hours after administration. The volume of the samples (usually 1-1.5 mL) was determined by weighing the collection tubes before and after the blood sampling using a precision scale and assuming a blood density of 1.06 g/mL. Activity concentration in each sample was counted as MBq/mL using a gamma counter (Perkin Elmer, Wizard²) and used as a proxy of the tracer concentration in circulation. Blood activities were fit to a biphasic model and alpha- and beta-phase half-lives reported for each patient.

Biodistribution and Image Analysis

The 99mTc-PHC-102 SPECT/CT images were assessed visually and quantitatively by evaluating the tumor lesions as well as the healthy organ biodistribution and radiation dosimetry. Biodistribution was determined as the fraction of injected activity (FIA) normalized to estimated organ or lesion weight as a function of time from administration for each lesion and healthy organ. Organ and lesion weights were estimated from volume assuming a density of 1.0. Absorbed effective radiation doses was calculated according to the Olinda methodology, using software package (Hybrid Viewer 4.0 Dosimetry, Hermes Medical) for specific effective organ doses. Blood samples were used to assess bone marrow dosimetry. Lesion volumes were determined on the CT images acquired during the SPECT/CT scans. Volumes of interest (VOI) were drawn manually around organs. A maximum tolerated total radiation burden was set at 10 mSv.

Safety Monitoring

For all participants, the safety of 99mTc-PHC-102was evaluated based on laboratory parameters (Supplementary Table 1), vital signs, electrocardiograms, and physical examinations before and up to 6 hours after intravenous administration of the radiotracer, and again during the follow-up visit (8 days after administration). Adverse events were continuously recorded.

Statistical Analysis

No statistical hypotheses were tested in the study, and the determination of the sample size is not applicable. Descriptive statistics were provided for dosimetry of lesions and healthy organs considering the Specific Absorbed dose (mSv/MBq) and the Estimated dose (Gy) as well as pharmacokinetic parameters. Incidence for any adverse events was calculated considering severity and MedDra classification with System Organ Class and Preferred Term, together with vital signs, abnormal laboratory values and physical examinations.

RESULTS

Radiolabeling Procedure

Incorporation procedure of 99mTc into the unlabeled precursor (PHC-101) was optimized to obtain radiochemical purity of ≥95% and specific activity of ≥23 MBq/µg. 99mTc-PHC-102 for injection was freshly prepared prior to each injection (Supplementary Table 2). Dose adjustment to 50 µg CAIX ligand was performed by dilution of the prepared 99mTc-PHC-102 dose (600-800 MBq) with a solution of PHC-101.

Disposition of Subjects and Safety Assessment

Five patients with ccRCC were enrolled in the study. This study was conducted at the Department for Biomedical Imaging and Image-guided Therapy, Division of Nuclear Medicine, Medical University in Vienna. The patients received the study drug and were imaged by SPECT/CT at multiple time points. Two patients with metastatic disease and three patients with primary RCC were enrolled. Characteristics of patients enrolled are shown in Table 1.

All 5 patients enrolled were evaluable for safety analysis. 99mTc-PHC-102 (50 µg total CAIX ligand, 600-800 MBq) was well tolerated and no clinically relevant adverse events were recorded. Haematological parameters were also not affected (Supplementary Table 1).

Biodistribution and Pharmacokinetics of 99mTc-PHC-102

A dosimetric analysis revealed an overall effective dose per patient of 6.3 ± 1.7 mSv (Supplementary Table 3). The organ specific standardised uptake values (SUV_{max} and SUV_{mean}) at 30 minutes, 2 hours and 6 hours post injection are shown in Table 2.

A pharmacokinetic analysis (Figure 1), based on radioactive counting of blood specimens at multiple time points, revealed a biphasic clearance profile with a fast $t_{1/2}$ = 0.1361 hours, corresponding to 55.0% of the clearance profile, and a slow $t_{1/2}$ = 1.35, corresponding to the remaining 44.9% of the clearance profile [25].

Imaging Results

Patient 1 (a 80 year old male) has been diagnosed with CAIX positive clear cell renal cell carcinoma after accusing abdominal discomfort and haematuria for several months. At the time of the diagnosis the patient already presented lymph node metastasis. A 7.2 cm lesion in the left kidney was clearly visible 6 hours after injection of 99mTc-PHC-102 both in whole-body planar and transverse 99mTc-PHC-102 SPECT/CT scan (Figure 2A and 2B). Radiotracer uptake in stomach and in the gallbladder was also observed, in line with published CAIX expression patterns. Surprisingly, a previously unknown pulmonary metastatic lesion of 2.3 cm in the right upper lobe was also detected at all imaging time points (0.5, 2 and 6 hours) (Figure 2C).

Patient 2 (a 68 year old male) was admitted to the hospital for a perforated appendicitis. A native CT showed a 2.5 cm lesion in the upper kidney pole. A later conducted MRI with arterial enhancement showed a RCC-suspect lesion. Biopsy results confirmed a positive RCC. CAIX was positive only in isolated cells. In the 99mTc-PHC-102 SPECT/CT scan the lesion protruding from the cortex of the right kidney was detectable at all time points (Figure 3).

Patient 3 (a 80 year old male) had an already diagnosed ccRCC with lymph nodes metastases. The 99mTc-PHC-102 SPECT/CT scan shows physiological uptake in the stomach and gut. Moreover, there is an inhomogeneous tracer accumulation in the right renal bed, assignable to the extended tumor mass. At the admission timepoint a tumor mass was detectable in the vena cava.

Here we show a 99mTc-PHC-102 uptake in the vena cava inferior correspondent to the intra-venous tumor mass. Interestingly, focal 99mTc-PHC-102 uptake was observed in the left upper lung lobe, not previously described in CT reports (Figure 4).

Patient 4 (a 49 year old male) presented with haematuria for a routine check-up. A kidney ultrasound revealed 1.9 cm kidney lesion in the hilum. Biopsy results showed a CAIX positive ccRCC. The 99mTc-PHC-102 SPECT/CT scan reveals a hilum lesion with low traceruptake at all imaging time points.

Patient 5 (a 32 year old male) was in treatment at a fertility clinic. A routine urine examination showed microhaematuria. A CT examination showed a 3.5 cm lesion in the lower left kidney pole, which turned out to be a ccRCC in histology. The 99mTc-PHC-102 SPECT/CT scan revealed a weak traceraccumulation at all imaging time points.

DISCUSSION

In this study we have shown that ccRCC patients can safely be imaged using 99mTc-PHC-102 SPECT/CT. The methodology is easy to implement in routine clinical practice and provides valuable information like uptake in primary lesions and detection of previously unknown metastatic lesions.

CAIX is physiologically expressed in stomach, small intestine and gallbladder. Small molecules reach those structures *in vivo* more efficiently than antibodies, reflecting a higher extravasation rate and easier diffusion into tissues [13]. We have previously reported that stomach and kidney uptake values decrease at higher doses of PHC-102, with a possible benefit for both imaging and therapy applications [6]. The uptake quantification reported in this first microdosing study compare well with those reported for other successful radiopharmaceuticals (e.g. PSMA ligands) [26]. Thus, it is possible that PHC-102 analogues, labeled with an alpha or a beta-emitting radionuclide, may be suitable for radionuclide therapy.

The detection of metastatic lesions has a particular medical value in ccRCC patients. While early-stage patients with localized tumors typically undergo surgical intervention [27], systemic administration of VEGFR inhibitors, TKIs, anti-PD-1 and anti-PD-L1 antibodies represent preferred treatment options for metastatic ccRCC [28]. It would be interesting to perform a side-by-side comparison for the imaging of metastatic lesions with 99mTc-PHC-102 and conventional radiotracers (e.g., 2-[^{18}F]fluoro-2-deoxy-D-glucose), as application of [^{18}F]FDG PET/CT showed limitations for ccRCC detection, due to the physiological excretion of [^{18}F]FDG through the kidneys, which decreases contrast between healthy tissue and neoplastic lesions [29-31].

Our results suggest that CAIX-lesions can efficiently be targeted with acetazolamide derivates in patients with localized or metastatic ccRCC. We have previously shown that acetazolamide-based small molecule-drug conjugates (SMDC) target CAIX-positive tumors more efficiently than their antibody-drug conjugate (ADC) counterpart [12]. Indeed, SMDC products may be ideally suited for the selective delivery of potent cytotoxic agents, such as monomethylauristatin E [10, 12]. SMDCs synergize with tumor-targeting antibody-interleukin-2 fusions [11]. Recombinant human interleukin-2 is approved for the treatment of metastatic renal cell carcinoma [32, 33] and it appears that the antibody-based delivery of this cytokine to the tumor side may potentiate activity while helping spare normal tissues [34-36]. In this context,99mTc- PHC-102 may represent a useful companion diagnostic for the clinical development of CAIX-specific SMDCs, in full analogy to what previously implemented by scientists at Endocyte for the molecular targeting of folate receptor [37-39] and of PSMA [40, 41].

In summary, our data shows that 99mTc-PHC-102 appears to be well suited for the molecular imaging of CAIX-positive clear cell renal cell carcinomas. SPECT/CT procedures reveal anatomical localization of primary and metastatic lesions and may be easier to implement compared to PET analysis, in terms of scanner accessibility and ease of radioactive labeling. The possibility of imaging patients a few hours after intravenous administration of the radiotracer should facilitate the routine implementation of 99mTc-PHC-102 methodologies, as compared to similar procedures based on monoclonal antibodies, which also gave excellent imaging results but at later time points and with a higher radiation burden for the patients. The successful imaging of ccRCC lesions (including previously unknown metastatic masses) provides a motivation to continue studying the tumor-targeting properties of 99mTc-PHC-102 at higher doses and in a variety of different CAIX-positive tumors (e.g., colorectal and urothelial cancer). Future studies will show whether 99mTc-

PHC-102 can also detect antigen-positive lesions in other tumor types (e.g., colorectal cancer, urothelial cancer, high-grade astrocytomas), which are known to express CAIX [42].

ACKNOWLEDGMENTS

The authors would like to thank Sabrina Matschitsch and Markus Raidl for excellent technical support. This project has received funding from the European Community under the grant agreement number E!9669 (ATRI). D.N. was supported by ETH Zurich. This project has received funding from the Swiss National Science Foundation (Grant Nr. 310030_182003/1) and the European Research Council (ERC) under the European Union's Horizon 2020 research and innovation program (grant agreement 670603).

KEY POINTS

Question

Can 99mTc-PHC-102, a novel CAIX-targeted radiotracer, be used for diagnostic purposes to detect primary tumors and metastatic lesions in patients with RCC?

Pertinent Findings

Our microdosing results in five RCC patients confirmed that 99mTc-PHC-102 localizes in primary tumors, with favourable tumour-to-background ratios. 99mTc-PHC-102 -SPECT/CT allowed the identification of previously unknown lung and lymph node metastases in two patients.

Implications for Patient Care

99mTc-PHC-102 is a promising SPECT tracer for the imaging of patients with clear cell renal cell carcinoma, with the potential to identify primary and metastatic lesions in different anatomical locations.

REFERENCES

1. Supuran CT. Inhibition of carbonic anhydrase IX as a novel anticancer mechanism. *World J Clin Oncol*. 2012;3:98-103.
2. Takacova M, Bartosova M, Skvarkova L, et al. Carbonic anhydrase IX is a clinically significant tissue and serum biomarker associated with renal cell carcinoma. *Oncol Lett*. 2013;5:191-7.
3. Uhlen M, Bjorling E, Agaton C, et al. A human protein atlas for normal and cancer tissues based on antibody proteomics. *Mol Cell Proteomics*. 2005;4:1920-32.
4. Bui MH, Seligson D, Han KR, et al. Carbonic anhydrase IX is an independent predictor of survival in advanced renal clear cell carcinoma: implications for prognosis and therapy. *Clin Cancer Res*. 2003;9:802-11.
5. Wang Y, Wang XY, Subjeck JR, Kim HL. Carbonic anhydrase IX has chaperone-like functions and is an immunoadjuvant. *Mol Cancer Ther*. 2008;7:3867-77.
6. Krall N, Pretto F, Mattarella M, Muller C, Neri D. A technetium 99m-labeled ligand of carbonic anhydrase IX selectively targets renal cell carcinoma in vivo. *J Nucl Med*. 2016;57:943-9.
7. Cazzamalli S, Dal Corso A, Neri D. Acetazolamide serves as selective delivery vehicle for dipeptide-linked drugs to renal cell carcinoma. *Mol Cancer Ther*. 2016;15:2926-35.
8. Krall N, Pretto F, Decurtins W, Bernardes GJ, Supuran CT, Neri D. A small-molecule drug conjugate for the treatment of carbonic anhydrase IX expressing tumors. *Angew Chem Int Ed Engl*. 2014;53:4231-5.
9. Krall N, Pretto F, Neri D. A bivalent small molecule-drug conjugate directed against carbonic anhydrase IX can elicit complete tumour regression in mice. *Chem Sci*. 2014;5:3640-4.
10. Cazzamalli S, Corso AD, Neri D. Linker stability influences the anti-tumor activity of acetazolamide-drug conjugates for the therapy of renal cell carcinoma. *J Control Release*. 2017;246:39-45.
11. Cazzamalli S, Ziffels B, Widmayer F, et al. Enhanced therapeutic activity of non-internalizing small-molecule-drug conjugates targeting carbonic anhydrase IX in combination with targeted Interleukin-2. *Clin Cancer Res*. 2018;24:3656-67.
12. Cazzamalli S, Dal Corso A, Widmayer F, Neri D. Chemically defined antibody- and small molecule-drug conjugates for in vivo tumor targeting applications: a comparative analysis. *J Am Chem Soc*. 2018;140:1617-21.

13. Divgi CR, Pandit-Taskar N, Jungbluth AA, et al. Preoperative characterisation of clear-cell renal carcinoma using iodine-124-labelled antibody chimeric G250 (124I-cG250) and PET in patients with renal masses: a phase I trial. *Lancet Oncol*. 2007;8:304-10.

14. Divgi CR, Uzzo RG, Gatsonis C, et al. Positron emission tomography/computed tomography identification of clear cell renal cell carcinoma: results from the REDECT trial. *J Clin Oncol*. 2013;31:187-94.

15. Dennis MS, Jin H, Dugger D, et al. Imaging tumors with an albumin-binding Fab, a novel tumor-targeting agent. *Cancer Res*. 2007;67:254-61.

16. Yuan F, Dellian M, Fukumura D, et al. Vascular permeability in a human tumor xenograft: molecular size dependence and cutoff size. *Cancer Res*. 1995;55:3752-6.

17. Peeters SG, Dubois L, Lieuwes NG, et al. [(18)F]VM4-037 microPET imaging and biodistribution of two in vivo CAIX-expressing tumor models. *Mol Imaging Biol*. 2015;17:615-9.

18. Dubois L, Lieuwes NG, Maresca A, et al. Imaging of CA IX with fluorescent labelled sulfonamides distinguishes hypoxic and (re)-oxygenated cells in a xenograft tumour model. *Radiother Oncol*. 2009;92:423-8.

19. Doss M, Kolb HC, Walsh JC, et al. Biodistribution and radiation dosimetry of the carbonic anhydrase IX imaging agent [(18) F]VM4-037 determined from PET/CT scans in healthy volunteers. *Mol Imaging Biol*. 2014;16:739-46.

20. Wichert M, Krall N, Decurtins W, et al. Dual-display of small molecules enables the discovery of ligand pairs and facilitates affinity maturation. *Nat Chem*. 2015;7:241-9.

21. Low EV, Avery AJ, Gupta V, Schedlbauer A, Grocott MP. Identifying the lowest effective dose of acetazolamide for the prophylaxis of acute mountain sickness: systematic review and meta-analysis. *BMJ*. 2012;345:e6779.

22. Liu S, Edwards DS, Barrett JA. 99mTc labeling of highly potent small peptides. *Bioconjug Chem*. 1997;8:621-36.

23. Fisher RE, Siegel BA, Edell SL, et al. Exploratory study of 99mTc-EC20 imaging for identifying patients with folate receptor-positive solid tumors. *J Nucl Med*. 2008;49:899-906.

24. Barrett JA, Coleman RE, Goldsmith SJ, et al. First-in-man evaluation of 2 high-affinity PSMA-avid small molecules for imaging prostate cancer. *J Nucl Med*. 2013;54:380-7.

25. Borsi L, Balza E, Bestagno M, et al. Selective targeting of tumoral vasculature: comparison of different formats of an antibody (L19) to the ED-B domain of fibronectin. *Int J Cancer*. 2002;102:75-85.

26. Afshar-Oromieh A, Malcher A, Eder M, et al. PET imaging with a [68Ga]gallium-labelled PSMA ligand for the diagnosis of prostate cancer: biodistribution in humans and first evaluation of tumour lesions. *Eur J Nucl Med Mol Imaging*. 2013;40:486-95.

27. Escudier B, Porta C, Schmidinger M, et al. Renal cell carcinoma: ESMO Clinical Practice Guidelines for diagnosis, treatment and follow-up. *Ann Oncol*. 2016;27:v58-v68.

28. Rodriguez-Vida A, Hutson TE, Bellmunt J, Strijbos MH. New treatment options for metastatic renal cell carcinoma. *ESMO open*. 2017;2:e000185.

29. Wang HY, Ding HJ, Chen JH, et al. Meta-analysis of the diagnostic performance of [18F]FDG-PET and PET/CT in renal cell carcinoma. *Cancer Imaging*. 2012;12:464-74.

30. Aide N, Cappele O, Bottet P, et al. Efficiency of [(18)F]FDG PET in characterising renal cancer and detecting distant metastases: a comparison with CT. *Eur J Nucl Med Mol Imaging*. 2003;30:1236-45.

31. Miyakita H, Tokunaga M, Onda H, et al. Significance of 18F-fluorodeoxyglucose positron emission tomography (FDG-PET) for detection of renal cell carcinoma and immunohistochemical glucose transporter 1 (GLUT-1) expression in the cancer. *Int J Urol*. 2002;9:15-8.

32. Amin A, White RL. Interleukin-2 in renal cell carcinoma: a has-been or a still-viable option? *J Kidney Cancer VHL*. 2014;1:74-83.

33. Rosenberg SA, Yang JC, Topalian SL, et al. Treatment of 283 consecutive patients with metastatic melanoma or renal cell cancer using high-dose bolus interleukin 2. *JAMA*. 1994;271:907-13.

34. Carnemolla B, Borsi L, Balza E, et al. Enhancement of the antitumor properties of interleukin-2 by its targeted delivery to the tumor blood vessel extracellular matrix. *Blood*. 2002;99:1659-65.

35. Johannsen M, Spitaleri G, Curigliano G, et al. The tumour-targeting human L19-IL2 immunocytokine: preclinical safety studies, phase I clinical trial in patients with solid tumours and expansion into patients with advanced renal cell carcinoma. *Eur J Cancer*. 2010;46:2926-35.

36. Eigentler TK, Weide B, de Braud F, et al. A dose-escalation and signal-generating study of the immunocytokine L19-IL2 in combination with dacarbazine for the therapy of patients with metastatic melanoma. *Clin Cancer Res*. 2011;17:7732-42.

37. Leamon CP, Parker MA, Vlahov IR, et al. Synthesis and biological evaluation of EC20: a new folate-derived, (99m)Tc-based radiopharmaceutical. *Bioconjug Chem*. 2002;13:1200-10.

38. Pribble P, Edelman MJ. EC145: a novel targeted agent for adenocarcinoma of the lung. *Expert Opin Investig Drugs*. 2012;21:755-61.

39. Naumann RW, Coleman RL, Burger RA, et al. PRECEDENT: a randomized phase II trial comparing vintafolide (EC145) and pegylated liposomal doxorubicin (PLD) in combination versus PLD alone in patients with platinum-resistant ovarian cancer. *J Clin Oncol*. 2013;31:4400-6.
40. Wang J, Zang J, Wang H, et al. Pretherapeutic 68Ga-PSMA-617 PET may indicate the dosimetry of 177Lu-PSMA-617 and 177Lu-EB-PSMA-617 in main organs and tumor lesions. *Clin Nucl Med*. 2019;44:431-8.
41. Rathke H, Giesel FL, Flechsig P, et al. Repeated (177)Lu-labeled PSMA-617 radioligand therapy using treatment activities of up to 9.3 GBq. *J Nucl Med*. 2018;59:459-65.
42. Wykoff CC, Beasley NJ, Watson PH, et al. Hypoxia-inducible expression of tumor-associated carbonic anhydrases. *Cancer Res*. 2000;60:7075-83.

FIGURES

Figure 1

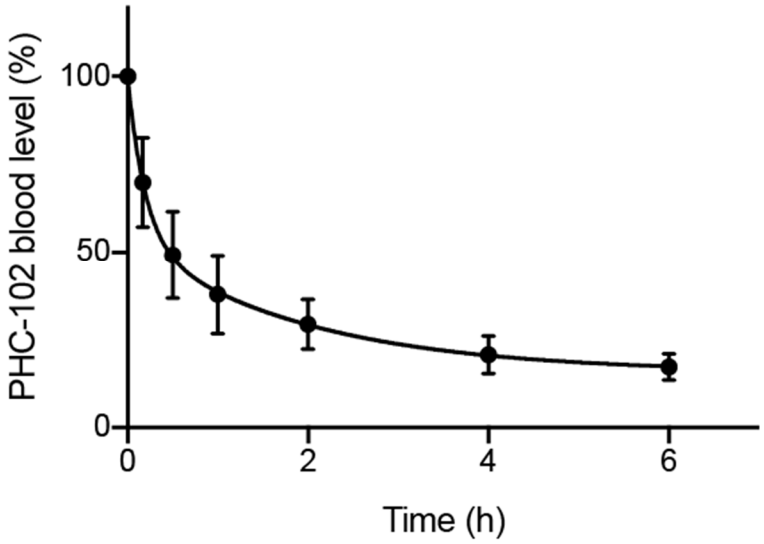

Legend 99mTc-PHC-102 blood levels. Blood clearance profiles were assessed by collecting blood samples at different time points and by counting the corresponding radioactivity values. The curve was calculated as an average of values derived from the individual patients. Variations in clearance rates were observed which might reflect differences in kidney function.

Figure 2

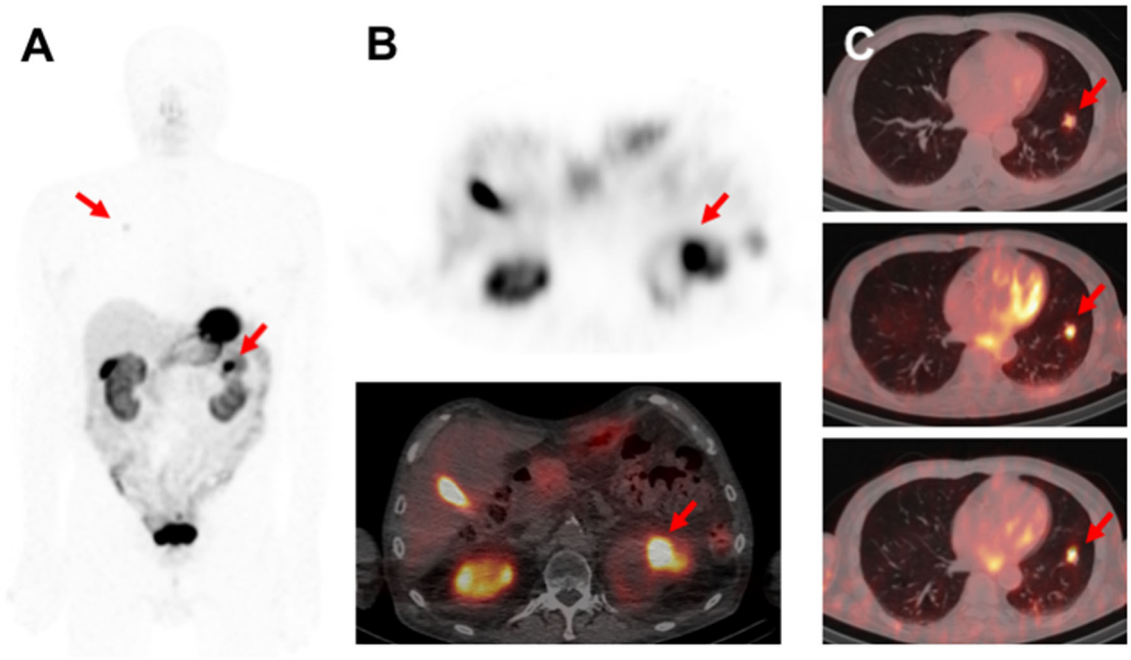

Legend (A) Anterior whole-body planar and (B, C) transverse SPECT/99mTc-PHC-102 images in 80 year old patient with clear cell renal cell carcinoma (CAIX positive). High uptake of the radio-tracer in the primary tumor (7.2 cm upper kidney pole left), in the stomach and in the gallbladder was observed. An additional metastatic lesion (2.3 x 1.6 cm) in the lung was also detected at all time points (0.5, 2 and 6 hours).

Figure 3

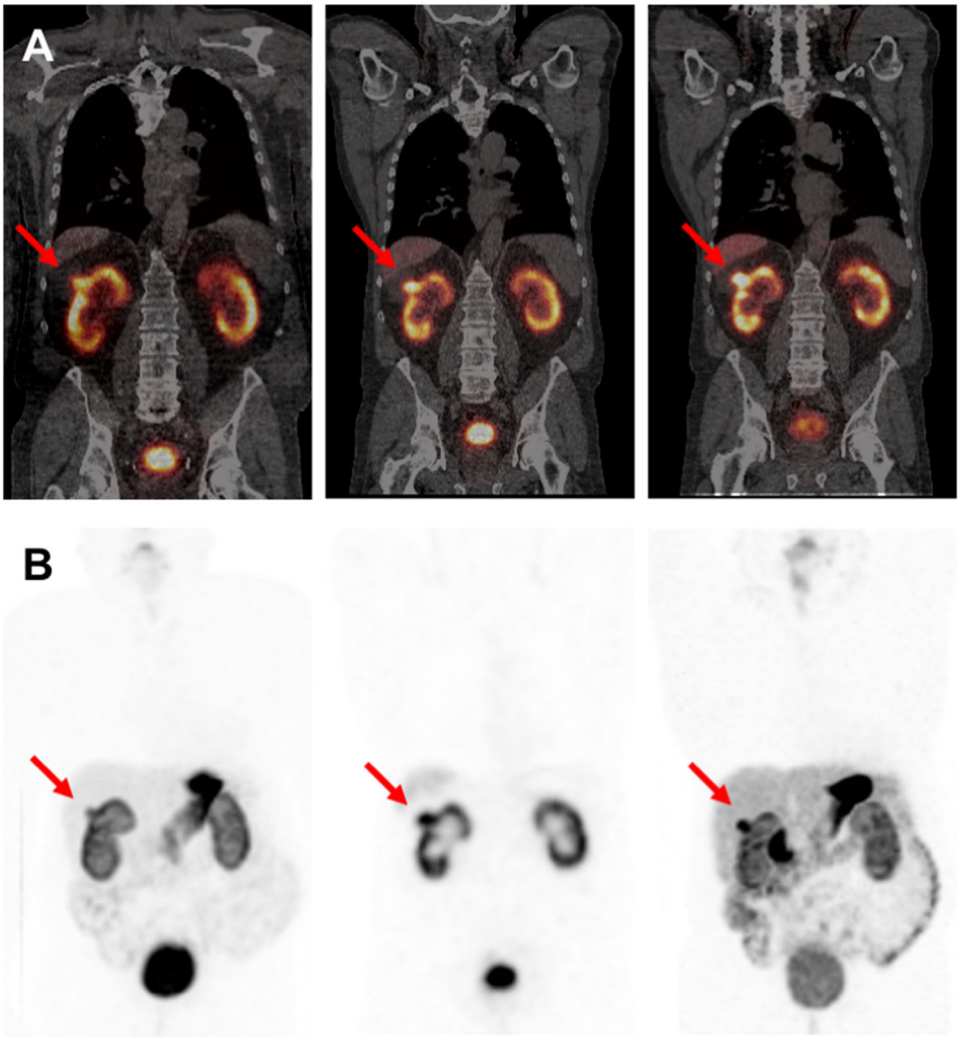

Legend Anterior (A) SPECT/CT and (B) SPECT scans obtained with 99mTc-PHC-102 in a 49 year old patient, 30 min, 2 and 6 hours after administration of the tracer (from left to right, respectively). The primary neoplastic lesion protruding from the cortex of the right kidney (1.6 cm) is visible at all time points. Renal excretion is appreciable from the high signal observed in the bladder at the 30 min time point and from the kidney uptake.

Figure 4

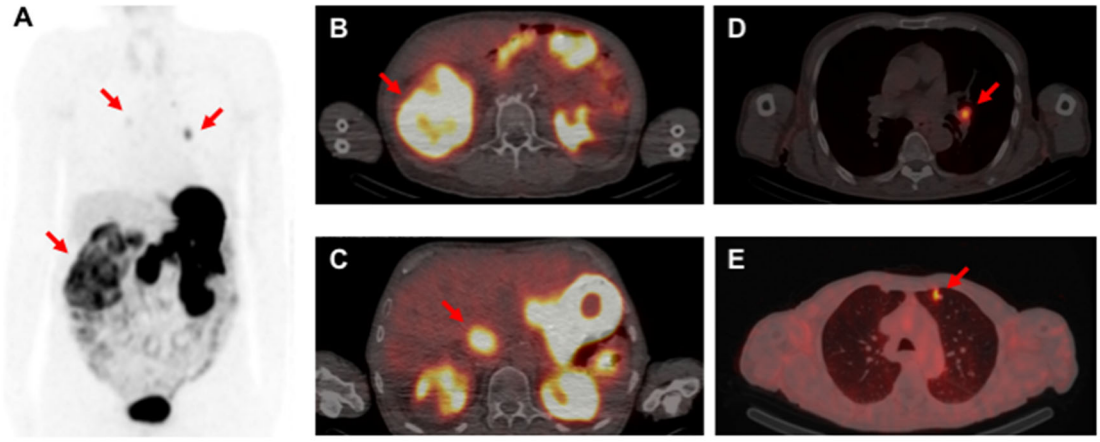

Legend Anterior (A) SPECT and (B) transverse SPECT/CT scans obtained with 99mTc-PHC-102 in an 80 year old patient at the 6-hour time point. The primary large tumour mass (A, B) present in the right kidney (7.2 cm) was detectable as consequence of high tracer uptake. A tumor thrombus in the vena cava (B, C) as well as metastatic lesions in a lymph node (D) and in the lung (E) were also visible 6 hours after 99mTc-PHC-102 injection as a consequence of high uptake of the tracer.

TABLES

Table 1

Subject	Age (years)	Gender (M/F)	Duration of disease (years)	Histology – CA IX
1	80	M	<2	positive
2	68	M	<2	positive
3	80	M	<2	positive
4	49	M	<2	negative
5	32	M	<2	unknown

Legend Demographic parameters and histological information of the study population.

Table 2

Organ	SUV_{max}			SUV_{mean}		
	30 min	**2 h**	**6 h**	**30 min**	**2 h**	**6 h**
Tumor	20.14±3.94	18.43±5.15	15.48±4.74	14.02±3.32	11.7±3.08	10.38±2.07
Kidney	35.04±6.50	26.6±4.05	17.50±2.19	19.68±4.49	16.75±1.75	12.24±1.33
Liver	4.26±1.13	5.43±1.11	6.06±3.08	3.1±1.16	4.00±1.14	4.54±2.57
Gallbladder	9.23±3.66	17.2±6.58	28.58±11.80	6.55±2.48	10.65±2.77	15.28±3.99
Intestine	6.78±1.03	11.3±4.57	10.80±3.39	3.44±1.12	3.65±0.60	3.04±0.93
Lung	0.94±0.32	0.85±0.30	0.56±0.26	0.58±0.26	0.40±0.27	0.22±0.13
Brain	0.32±0.15	0.375±0.22	0.28±0.17	0.12±0.12	0.11±0.13	0.06±0.05
Stomach	47.68±15.63	58.5±16.42	49.18±28.54	21.22±5.93	24.88±6.12	20.96±8.14
Spleen	1.28±0.29	0.925±0.34	0.78±0.13	0.62±0.26	0.35±0.21	0.22±0.08
Salivary Gland	3.02±2.52	1.32±2.38	1.60±0.94	2.3±1.69	1.83±1.31	1.08±0.64

Legend 99mTc-PHC-102 standardised uptake values corresponding to the 30-minutes, 2-hour and 6-hour time points. Average SUV max and mean are calculated based on individual values from the 5 patients imaged with microdosing 99mTc-PHC-102 SPECT/CT.

Supplementary Tables

Supplementary Table 1

	Average - Baseline	Average - After PHC-102 SPECT/CT	Reference values	Units
Blood Count				
Erythrocytes	4.1	3.9	4.4 - 5.8	T/L
Hemoglobin	11.8	11.2	13.5 - 18.0	g/dL
Hematocrit	34.5	32.7	40.0 - 52.0	%
MCV	84.6	84.2	78.0 - 98.0	fL
MCH	28.9	28.8	27.0 - 33.0	pg
MCHC	34.2	34.2	30.0 - 36.0	g/dL
Erythrocytes (Fraction)	14.0	13.8	11.0 - 16.0	%
Platelets	202.8	226.4	150 - 350	G/L
Mean Platelets Volume	11.3	11.1	7.0 - 13.0	fL
Leukocytes	7.6	8.9	4.0 - 10.0	G/L
Differential Count				
Neutrophiles (absolut)	4.0	6.2	2.0 - 7.5	G/L
Neutrophiles (relative)	61.2	71.1	50.0 - 75.0	%
Lymphocytes (absolut)	1.7	1.4	1.0 - 4.0	G/L
Lymphocytes (relative)	26.8	16.9	25.0 - 40.0	%
Monocytes (absolut)	0.6	0.8	0.0 - 1.2	G/L
Monocytes (relative)	8.2	9.0	0.0- 12.0	%
Eosinophils (absolut)	0.2	0.2	0.0 - 0.4	G/L
Eosinophils (relative)	3.3	2.6	0.0 - 4.0	%
Basophils (absolut)	0.0	0.0	0.0 - 0.1	G/L
Basophils (relative)	0.5	0.5	0.0 - 1.0	%
aPTT	39.1	36.1	27.0 - 41.0	s
Fibrinogen - Clauss	488.0	391.0	200 - 400	mg/dL
Clinical Chemistry				
Sodium	140.3	137.7	136 - 145	mmol/L
Potassium	4.7	4.4	3.5 - 5.1	mmol/L
Chloride	99.6	99.0	98 - 107	mmol/L
Calcium	6.3	2.2	2.20 - 2.55	mmol/L
Inorganic Phosphate	1.2	1.2	0.81 - 1.45	mmol/L
Magnesium	1.0	1.1	0.66 - 1.07	mmol/L
Creatinine	0.9	1.0	0.70 - 1.20	mg/dL
Urea	15.4	14.9	8.0 - 23.0	mg/dL
Bilirubin (total)	2.1	2.1	0.0 - 1.2	mg/dL
Hemoglobin (free)	45.0	33.8	< 4	mg/dL
Albumin	41.8	37.0	35.0 - 52.0	g/L
ASAT (GOT)	41.2	17.3	< 50	U/L
ALAT (GPT)	38.8	27.8	< 50	U/L
Gamma - GT	59.2	35.8	< 60	U/L

Laboratory parameters before and after PHC-102 SPECT/CT microdosing procedure. Overall profile was not altered by administration of PHC-102 as evident by the comparison of blood count and clinical chemistry values calculated as average of data available from the five patients imaged.

Supplementary Table 2

Batch	Purity HPLC [%]	Purity TLC [%]	Starting activity [MBq]	Activity product [MBq]	Specific activity [MBq/µg]*
I	95.2	99.76	2070	1450	29
II	99.86	98.88	1400	1030	20.6
III	95.1	99.57	1150	954	19.08
IV	94.5	97.08	1570	1299	25.98
V	93.7	100	1950	1132	22.64
Average	95.672	99.058	1628	1173	23.46

Radiochemical incorporation and specific activity prior dilution of each different PHC-102 batch (each different batch corresponds to material prepared for each different patient imaged with PHC-102 SPECT/CT procedure). The product solution was diluted with a cold PHC-101 solution to obtain a final activity of 800 MBq/50µg.

Supplementary Table 3

Target Organ	ICRP-103 ED - Patient 1	ICRP-103 ED - Patient 2	ICRP-103 ED - Patient 3	ICRP-103 ED - Patient 4	ICRP-103 ED - Patient 5
Brain	2.50E-02	1.17E-08	1.76E-02	5.96E-03	1.21E-04
Gallbladder Wall	9.00E-02	4.85E-01	3.32E-02	3.33E-02	1.20E-02
Small Intestine	4.46E-01	1.02E-01	1.53E-01	1.01E-01	1.22E-02
Stomach Wall	5.93E+00	8.49E+02	7.16E+00	4.49E+00	4.23E+00
Kidneys	2.81E-01	1.22E+00	3.54E-01	2.63E-01	2.23E-01
Liver	5.49E-01	6.45E+00	6.03E+00	2.15E-01	7.03E-02
Lung	5.58E-01	2.69E+01	3.78E-01	2.97E-01	1.79E-01
Salivary Glands	2.72E-02	8.68E-02	5.66E-02	7.40E-03	3.75E-04
Spleen	8.74E-02	4.89E+00	6.09E-02	5.32E-01	4.14E-02

Total absorbed dose (mSv) to each organ after presented for each individual patient imaged with PHC-102 SPECT/CT procedure. Calculations are based on data at the three time points studies (30 min, 2 hours and 6 hours after intravenous administration of PHC-102).